High-dimensional Variance based Logic for Reliable Communication at Near-zero Energy-per-bit

Sri Harsha Kondapalli and Shantanu Chakrabartty
Electrical and Systems Engineering, Washington University in St Louis
Email: {sriharshakondapalli, shantanu}@wustl.edu

February 8, 2019

Abstract

In variance-based logic (VBL), information is encoded by the change in the variance of a signal as opposed to the conventional mean-based logic (MBL) where the information is encoded by the change in the mean of the signal. In this paper, we compare the fundamental limits on the minimum energy per bit that can be achieved by VBL and MBL representations in high-dimensional signal space. We show that while for MBL representations, the trade-off between the energy-per-bit and the bit-error-rate (BER) is fundamentally constrained by the classical Shannon-limit, using VBL representations it is theoretically possible to achieve arbitrarily small BER while dissipating near zero energy-per-bit. This surprising result has been experimentally verified for Additive-white-Gaussian-Noise (AWGN) channels using Monte-Carlo simulations. We believe that high-dimensional VBL based encoding could provide a new approach for designing ultra-energy-efficient communication and sensing systems.

1 Introduction

There exists a trade-off between the energy required for transmitting information across a noisy communication channel and the reliability of correctly decoding the transmitted information. This trade-off manifests itself as the celebrated Shannon-limit [1] which determines the minimum energy-per-bit (E_b/N_o) required to achieve arbitrary small bit-error-rate (BER) for a specific type of communication channel. In this paper, we argue that an alternate signal representation can overcome this fundamental limit and theoretically achieve arbitrarily small BER while dissipating near zero energy-per-bit. The proposed approach is based on our previously reported variance-based logic (VBL) representation where the information bit is encoded as the change in signal variance [2]. This logic representation is contrary to the conventional mean-based logic (MBL) representation where the information is encoded as the change in the average or the mean of the signal parameter, for instance, amplitude, phase or frequency [3–5]. Both of

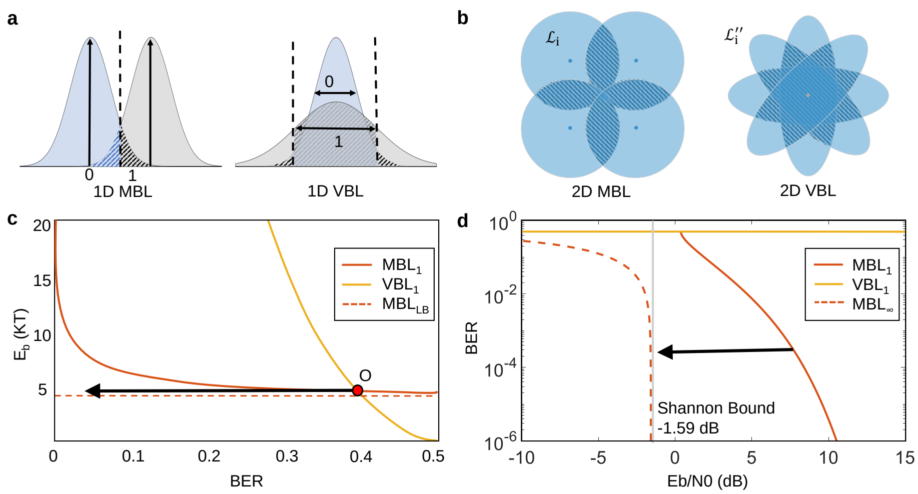

Figure 1: Comparison of MBL and VBL representations: (a) 1 dimensional (1D) and (b) 2 dimensional (2D) MBL and VBL code words $\mathcal{L}_i$ and $\mathcal{L}_i'$ with Gaussian pdfs respectively. (c) Comparison of thermodynamic energy-per-bit for 1-dimensional MBL and VBL as a function of average probability of error or BER; (d) BER-E_b/N_0 plots showing the Shannon-limit for MBL, and the proposal that using high-dimensional VBL it is possible to surmount this limit.

these representations are illustrated in Fig. 1(a) and (b) using one-dimensional (1D) and two-dimensional (2D) probability density functions (pdfs) where the overlap between the pdfs (shown as shaded regions) determines the probability-of-error (BER) for each of the respective representations. For a 1D MBL representation, we and others have shown that the thermodynamic energy dissipated per bit is bounded from below by 4KT Joules per bit and that this limit is achieved when the average probability of error approaches 0.5 or for high BER [6, 7]. However, in the case of 1D VBL it was shown in [6] that when the average probability of error approaches 0.5, the energy dissipated per bit goes to zero Joules per information bit. Both the trends are illustrated in Fig. 1(c) using a cross-over point O where one type of representation is shown to be more energy efficient than the other. Note that these lower-bounds only applies to the energy required to communicate across a noisy-channel and does not include the energy necessary for encoding and decoding at the source and the receiver respectively.

In this paper, we investigate the lower bounds on E_b/N_0 when using high-dimensional VBL (HD-VBL) representations. Specifically, we will investigate if the cross-over point (as shown in Fig. 1(c)) can be shifted towards the origin which would then imply that an HD-VBL representation could potentially achieve zero BER while dissipating near-zero amount of energy-per-bit. In the case of high-dimensional MBL (HD-MBL) lower bound on E_b/N_0 can be derived from Shannon's channel coding theorem, as summarized in Appendix 4.1, and is approximately equal to 0.6 or -1.6 dB for an additive white gaussian noise (AWGN) channel. Thus, all existing communication methods that use MBL representations are limited by this bound even when the dimensions used for encoding approaches infinity, as illustrated in Fig. 1(d). In the case of HD-VBL determining the fundamental limits on E_b/N_0 will involve understanding how the volume spanned by the overlap between the pdfs (as illustrated in Fig. 1(d)-(e) for 2D, 3D representation) scales as the number of dimensions become large.

Rest of the paper is organized as follows, section 2 presents a geometrical realization of high-dimensional VBL (HD-VBL) and derive the analytical expressions to estimate the BER and the capacity of HD-VBL. These results were validated using monte-carlo simulations. Brief discussions and conclusion of our work are provided in section. 3. Additional results are provided in the appendix. 4.

2 Analysis and Results of HD-VBL

We first present our analysis corresponding to a particular VBL representation that can be easily visualized. We follow a standard communication model, as shown in Fig. 2(a), comprising of a source that has access of M codewords, denoted by the set $\mathcal{L}$, which it needs to communicate over a noisy channel to a receiver. In the case of VBL, each codeword is encoded by modulating the variance of a zero-mean high-dimensional signal along a specific direction $v \in \mathbb{R}^D$ in a D-dimensional space. For an additive-white-Gaussian-noise (AWGN) channel, the codeword received at the receiver can be illustrated using the contours of a multi-dimensional Gaussian pdf that is geometrically represented using D-dimensional hyper-ellipsoids. When the channel is not being used, the received pdf at the receiver symmetrical and is illustrated using a D-dimensional hyper-sphere $\mathcal{S}_0$ and is determined by the noise spectral density (N_0). When the target codeword $\mathcal{L}_0$ is transmitted, the received pdf at the receiver is a hyper-ellipsoid $\mathcal{S}_1$ (as illustrated in Fig. 2(b)) whose major axis is oriented along the direction v. To detect whether the target code-word $\mathcal{L}_0$ was transmitted, the receiver uses a decoder whose decision boundaries coincide with two hyper-cylinders $\mathcal{T}_1$ and $\mathcal{T}_2$, as illustrated in Fig. 2(b). Both $\mathcal{T}_1$ and $\mathcal{T}_2$ are aligned along v (known a-priori) and terminated by spherical caps $\mathcal{C}_1$ and $\mathcal{C}_2$, formed by the overlap between hyper-ellipsoid $\mathcal{S}_1$ and the hyper-sphere $\mathcal{S}_0$. If the received noisy vector lies within the boundary of the hyper-cylinders, then the received vector is decoded as $\mathcal{L}_0$. Based on this decoder we can analytically estimate the probability-of-detection p_d of the code-word $\mathcal{L}_0$. Mathematically, we show in section 2.1, estimating the probability mass that lies within the decoding boundaries reduces to solving a two-fold hypothesis testing formulation involving χ^2 distributions. Then, for a given probability-of-detection p_d, we could estimate the number of non-overlapping spherical caps $\mathcal{C}_1$ and $\mathcal{C}_2$ that could be packed on the surface of the hyper-sphere $\mathcal{S}_0$, which gives us an estimate of the capacity of this specific VBL representation.

2.1 Estimation of BER for VBL with One Degree-of-Freedom

For a VBL with one degree of freedom, as illustrated in Fig. 2(b), the signal variance, corresponding to a code-word $\mathcal{L}_0$, is encoded along a D-dimensional vector. Without loss of generality, multi-dimensional variance could be represented using a diagonal

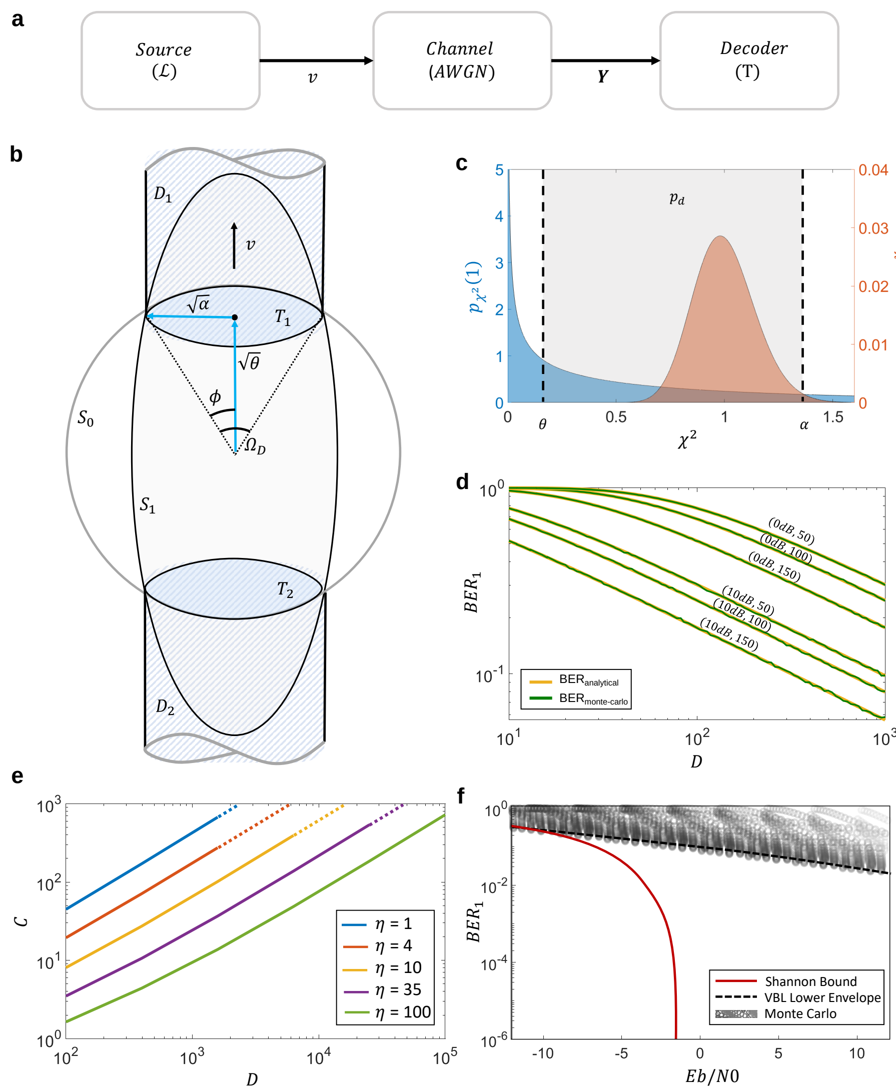

Figure 2: Estimation of capacity and BER for a one degree of freedom VBL representation and a specific type of decoder applied to (a) a general communication system. (b) Decision rule for estimating the probability of detection (p_d). (c) Estimation of BER reduced to a two-fold hypothesis testing based on a Chi-square distribution. (d) BER_1 with respect to number of dimensions (D) with parameters (SNR, θ). (e) Estimated channel capacity as a function of log(D) (f) BER_1-E_b/N_0 plot for the case $k = 1$.

covariance matrix (Σ_D) as,

$$\Sigma_D = [P + N_0,\ N_0,\ N_0, ...,\ N_0] \tag{1}$$

where P is the total signal power and N_0 is the channel noise power in each dimension. Thus, the multi-variate zero-mean normal distribution corresponding to the recieved vector $\mathbf{Y} = [y_1,\ y_2,\ ...,\ y_D]$ is given by,

$$f_Y(y_1, y_2, ...y_D) = A\ \exp\left(-\frac{1}{2}\left[\frac{y_1^2}{P + N_0} + \sum_{i=2}^{D}\frac{y_i^2}{N_0}\right]\right), \tag{2}$$

where A is the normalization factor. Note that this distribution can be parameterized using $[a,\ b] = \left[y_1,\ \sqrt{\left(\sum_{i=2}^{D}\frac{y_i^2}{D-1}\right)}\ \right]$ where each of the parameters a^2 and b^2 assumes a χ^2 distribution with 1 and $D-1$ degrees of freedom respectively. The respective χ^2 distributions with degrees of freedom 1 and $D-1$ are illustrated in Fig. 2(c). The decision rule (or decoder) is then determined by the solid angle Ω_D and ϕ in Fig. 2(b) and can be mapped into Fig. 2(c) as thresholds α and θ. The probability of detecting the codeword p_d is given by the total probability mass concentrated between the two thresholds, as shown in Fig. 2(c) and is given by

$$\begin{aligned}
p_d &= 1 - BER_1 = \mathbb{P}(\mathbf{Y} \in (\mathcal{T}_1 \cup \mathcal{T}_2)) \\
&= \mathbb{P}\left[(a^2 \geq \theta) \cup (b^2 \leq \alpha)\right] \\
&= \mathbb{P}\left[\left(\chi_1^2 \geq \frac{\theta}{P + N_0}\right) \cup \left(\chi_{D-1}^2 \leq \frac{(D-1)\alpha}{N_0}\right)\right] \\
&= \mathbb{P}\left[\left(\chi_1^2 \geq \frac{\theta'}{D\ SNR + 1}\right) \cup \left(\chi_{D-1}^2 \leq (D-1)\eta\theta'\right)\right] \\
&= \frac{\gamma(\frac{D-1}{2}, \frac{(D-1)\eta\theta'}{2})}{\Gamma(\frac{D-1}{2})}\left(1 - \frac{\gamma(\frac{1}{2}, \frac{\theta'}{2(D\ SNR+1)})}{\Gamma(\frac{1}{2})}\right)
\end{aligned} \tag{3}$$

Here $\theta' = \frac{\theta}{N_0}$ is the normalization parameter, $\eta = \frac{\alpha}{\theta} = (\tan\ \phi)^2$ and $SNR = \frac{P}{DN_0}$. Also, $\gamma(*, *)$ is the lower incomplete gamma function and $\Gamma(*)$ is the ordinary gamma function [8]. Fig. 2(d) shows the corresponding bit-error-rate BER_1, where the subscript corresponds to the VBL representation with one-degree of freedom. BER_1 asymptotically decreases with the increase in the number of dimensions D, for different levels of signal-to-noise ratio (SNR) and decoder parameters. Also, the analytical model for p_d has been validated using Monte-carlo simulations for multiple parameter realizations, as shown in Fig. 2(d).

To calculate the capacity of HD-VBL, we estimate the number of non-overlapping spherical caps that can be packed on the surface of a D-dimensional hyper-sphere determined the thresholds, as illustrated in Fig. 2(b). Estimation of optimal packing density for spherical-caps has been well studied in the context of spherical codes and in particular, wrapped spherical codes and laminated spherical codes [9]. The number of code words that can be accommodated in the space is given by the ratio between the total surface area, and the area spanned by one single codeword and is given by

$$M_1 = \frac{1}{I_{\sin^2(\tan^{-1}\sqrt{\eta})}\left(\frac{D-1}{2}, \frac{1}{2}\right)} \tag{4}$$

where $\eta = \frac{\alpha}{\theta}$. Details of the derivation can be found in the Appendix 4.2. Using the expression in equation 4, the capacity for this representation can be estimated as

$$C = \log_2 M_1 = \log_2\left(\frac{1}{I_{\sin^2(\tan^{-1}\sqrt{\eta})}\left(\frac{D-1}{2}, \frac{1}{2}\right)}\right). \tag{5}$$

Fig. 2(e) plots the capacity C with respect to the signal dimensions D, for different choices of the decoder hyper-parameters (θ, α, $\eta = \alpha/\theta$). The estimated capacity in equation 5 can be used to estimate the energy-per-bit ($\frac{E_b}{N_0}$) for a specific value of signal power P as

$$\frac{E_b}{N_0} = \frac{SNR}{C} \tag{6}$$

The results in Fig. 2(c) and (d) were used to obtain the BER_1-E_b/N_0 plot as shown in Fig 2(f). Note that every point in the VBL simulation in Fig 2(f) correspond to a specific choice of a decoder parameter set (θ, α). The result shows that for this VBL representation, the BER can be reduced, but at levels of energy-per-bit E_b/N_0 that are significantly higher than the theoretical Shannon-limit.

2.2 Estimation of BER for VBL with k-degrees-of-freedom

We now generalize the VBL representation to a topology where the variance is now encoded along a specific sub-manifold of dimension $k(< D)$, instead of a single direction or $k = 1$. The code-words are now represented by sub-manifolds that are spanned by a vectors $v' = [v_1, v_2, ...v_D]$, such that $\sum_{i=1}^{D} v_i = k$ with $v_i \in \{0, 1\}\ \forall\ i = [1, D]$. Similar to the analysis presented in section 2.1, the estimation of the modified parameters $[a_k,\ b_k] = \left[\sqrt{\left(\sum_{i=1}^{k} \frac{y_i^2}{k}\right)},\ \sqrt{\left(\sum_{i=k+1}^{D} \frac{y_i^2}{D-k}\right)}\ \right]$, which admits the pdfs $a_k^2 \sim \chi_k^2$ and $b_k^2 \sim \chi_{D-k}^2$. The respective distributions corresponding to $k = 3$ and $k = 10$ are shown in Fig. 3(a)-(b), where the respective probability-of-detections p_d^3 and $p_d^1 0$ are given by the total probability mass within the two thresholds θ and α.

Following similar arguments in section 2.1, the probability of decoding p_d^k can be estimated as

$$\begin{aligned} p_d^k &= 1 - BER_k = \mathcal{P}(\mathbf{Y} \in (\mathcal{T}_1' \cup \mathcal{T}_2')) \\ &= \frac{\gamma(\frac{D-k}{2}, \frac{(D-k)\eta\theta'}{2})}{\Gamma(\frac{D-k}{2})}\left(1 - \frac{\gamma(\frac{k}{2}, \frac{k\theta'}{2(D\ \frac{SNR}{k}+1)})}{\Gamma(\frac{k}{2})}\right) \end{aligned} \tag{7}$$

It can be seen in Fig. 3(b), as k increases the region signifying P_d spans a large proportion of the probability mass as depicted in the BER_k plots shown in Fig. 3(c)-(d). Note that sub-script k denotes the number of degrees-of-freedom considered in defining

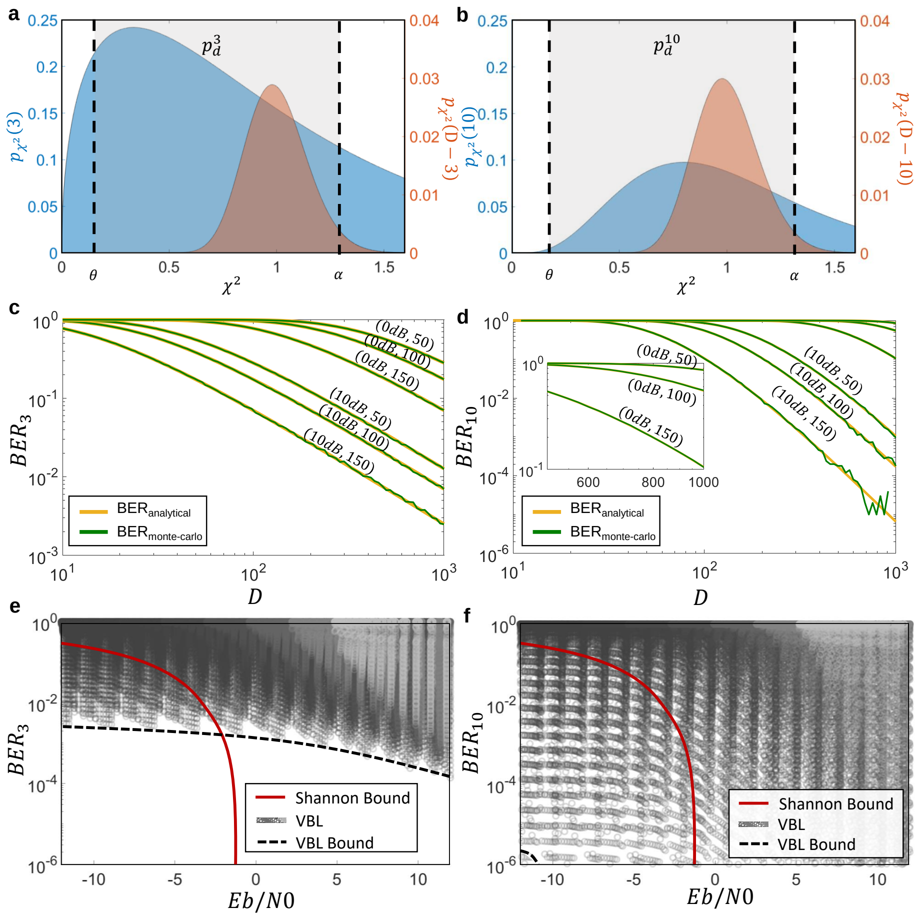

Figure 3: (a) (b) Estimation of the P_d using two-fold hypothesis testing for a 100 dimensional VBL representation with k=3, k=10 respectively. (c) (d) Verification of analytical BER expressions derived in equation. 3,7 with monte-carlo simulations for different parameter values (SNR, θ). (e) (f) Energy per bit $(EbN0)$ estimated as defined in equation. 6 vs BER plots for the case of VBL-HDL.

HD-VBL. The analytical results are given by equations 7 have also been verified using Monte-Carlo simulations, as shown in Fig. 3(c)-(d). Capacity for a VBL representation with k-degrees of freedom is estimated using spherical-cap packing techniques applied to a $D-k$ dimensional sphere as described in Appendix 4 and is given by

$$M_k = \frac{1}{I_{\sin^2\phi}\left(\frac{D-k}{2}, \frac{1}{2}\right)} \tag{8}$$

and capacity is given by,

$$C = \log_2 M_k = \log_2 \left(\frac{1}{I_{\sin^2(\tan^{-1}\sqrt{\eta})}\left(\frac{D-k}{2}, \frac{1}{2}\right)} \right) \tag{9}$$

The average bit-error rates (BER) and capacity (C) were computed for different thresholds (θ, α) and the energy per bit (E_b/N_0) was estimated using equation. 6 as described in the methods section. Fig. 3(e)-(f) show the BER-E_b/N_0 plots corresponding to the case $k = 3$ and $k = 10$. Again, each point in the BER simulation correspond to the results obtained for a specific choice of the decoder parameter θ, α. Also the limiting case of BER_{10} is shown in Fig. 4(d) which clearly shows the lower bound for the case of HD-MBL where E_b corresponding to HD-MBL approaching zero. The results clearly show that there exist HD-VBL representations for dimensions no more significant than 100, that can easily surpass the classical Shannon-limit. However, whether there exist VBL representations that can asymptotically achieve arbitrarily small BER at arbitrarily small $\frac{E_b}{N_0}$ still needs to be verified through extensive Monte-Carlo studies. This would require an exhaustive search over different decoding parameters and decoder topologies which in turn requires significant computational resources.

3 Discussion

The analysis and results presented in this paper seem to indicate that by encoding information in the variance of the signal we can surmount the limitation imposed by the classical Shannon-limit. The intuitive understanding of this effect is that VBL encodes information on the surface of a hyper-sphere, as shown in Fig. 2(b), whose volume asymptotically goes to zeros as the number of dimensions approaches infinity. As a result, for VBL the tails of the distributions project orthogonally to the hyper-spherical surface, as shown in Fig. 4(a), whereas the packing of the centroids is achieved on the surface of the hypersphere, as shown in Fig. 4(b). In a high-dimensional space and for low SNR, these two effects (packing and error rates) are not perfectly correlated and hence once could be reduced without reducing the other. For a conventional MBL representation, the Shannon-limit arises because the overlap between the pdfs of the adjacent codewords (centroids) lie within the volume spanned by their pdfs, as illustrated in Fig. 4(c). In higher dimensions and for a given signal-to-noise ratio, the packing density (or equivalently the channel capacity) scale linearly with the number of dimensions (as shown in the appendix section 4.1). As a result, the energy-per-bit $\frac{E_b}{N_0}$, cannot be further reduced while achieving near zero BER, thus leading to the Shannon-limit [10]. In terms of thermodynamic limits HD-VBL indeed moves the cross-over point O in

Fig. 1(c) towards the origin, which was the original motivation for this paper. This is clearly shown in Fig. 4(d) for different cases of VBL with 10-degrees of freedom and for dimensions $D = 100$.

One of the challenges in using VBL representation for practical communication system is the complexity in implementing the decoder at the receiver. While in this paper we showed that the asymptotic benefits hold for a simple VBL representation where the signal energy is directed towards modulating the variance along one direction (or axis), the convergence rates are slow and thus would require a large number of dimensions for encoding. We, therefore, extended the VBL representation by spreading the signal energy across variances along $k < D$ different directions. This clearly showed in Fig. 3(d) that such type of VBL encoding that surpasses the classical Shannon-limit. However, the optimality is achieved only when the correct set of decoding hyper-parameters are chosen. In appendix 4.3, we show how to choose the decoder parameters for a one-dimensional VBL representation. However, for higher-dimensional VBL and when multiple directions are chosen for encoding, one has to resort to an exhaustive search over the decoder parameter space to achieve the optimal decoding performance. Practical consideration and the complexity of the optimization procedure would impose limits on the correct choice of these parameters, however, note that for stationary channels, the parameters need to be estimated only once. Adaptive determination of the decoding hyper-parameters will be a topic of future research in this area. Also, note that even though we have shown the asymptotic property of near-zero BER at near-zero E_b/N_0 for a specific type of VBL representation, there might exist other VBL representations that might demonstrate superior convergence. In this spirit, there might exist some connection between VBL representations and stochastic resonance based decoding, where "noise" or variance is introduced into the system to improve the detection of a buried but harmonic signal [11]. Additionally, the practical realization of the VBL based communication system would be a topic for future research. In our original paper on VBL [6], we had highlighted that the energy-harvesting systems [2] and emerging valleytronic devices [12] could form a natural platform to implement some of the proposed communication techniques. Other approaches towards a practical realization of a VBL communication system could also involve exploiting the thermal-noise of electronic devices (resistors or transistors) to modulate the variance of the channel, as reported in [13, 14].

4 Appendix

4.1 Lower Bounds on $\frac{E_b}{N_0}$ for AWGN Channel.

The classical Shannon-limit has been estimated using the expression of channel-capacity for an AWGN channel. The limit on the K information bits that can be transmitted using a D dimensional signal and an average signal power of P over a channel with N_0

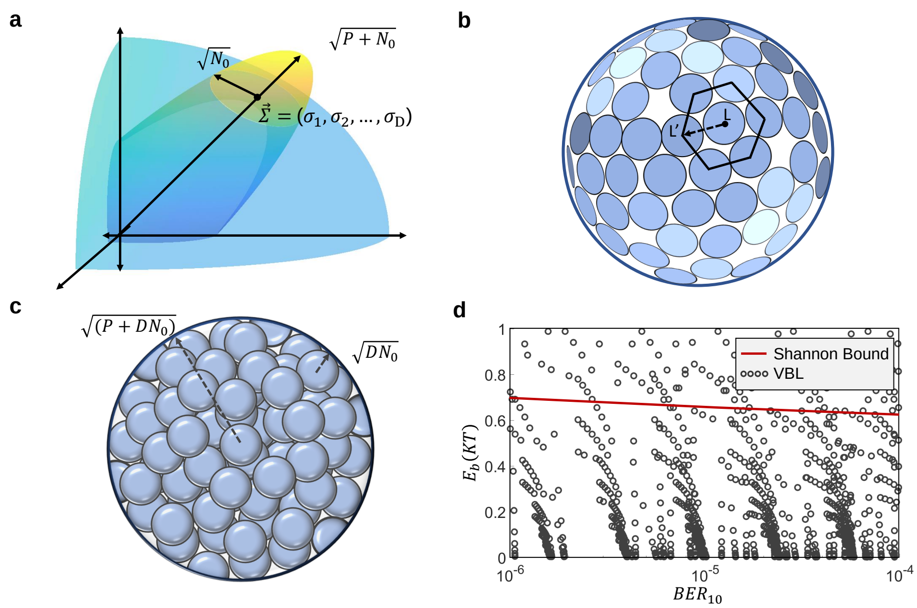

Figure 4: (a) Illustration of spherical cap and decoding cylinder oriented in the direction of vector v or variance vector defined by Σ (b) Surface Packing of high dimensional variance based codes and optimal packing density. (c) Sphere packing giving rise to the shannon bound on energy per bit (Eb/N_0) for reliable transmission of code words with signal power (P) over a noisy channel (N_0). (d) FOM plot indicating the region where VBL achieves encoding information with lower energy per bit than that of determined by the shannon bound.

noise power per dimension is given by,

$$\begin{aligned} K &< D\log_2(1+\frac{P}{N_0D}) \\ K &< D\log_2(1+\frac{E_bK}{N_0D}) \end{aligned} \tag{10}$$

Defining rate as $R = \frac{K}{D}$ gives,

$$R < \log_2(1+\frac{E_b}{N_0}R) \tag{11}$$

For a finite K and when dimensions $D \to \infty$, $R \to 0$. Thus,

$$\frac{E_b}{N_0} > \lim_{R\to 0}\frac{2^R-1}{R} = \ln 2 = 0.6931 = -1.59\ dB. \tag{12}$$

This is the absolute minimum amount of signal energy to noise power spectral density required to transmit at least one bit of information reliably. Similar lower-bound on E_b/N_0 can be arrived at by using sphere packing arguments presented in [10] and illustrated in Fig. 4(c).

4.2 Geometrical approach for finding capacity of VBL.

Firstly, we analyze for the case of HD-VBL with 1 degree-of freedom and later the results were extended for a much generic case (k DOF). As shown in section 2.1 the contours of a high dimensional pdf for a HD-VBL takes shape of an hyper-ellipsoid and the elapsed area on the surface decision boundary is given by a $D-1$ dimensional hyper sphere as shown in Fig. 4(a). Thus the maximum number of codewords (channel capacity) is be determined by counting the number of non overlapping $D-1$ hyper spheres on the surface of decision boundary as shown in 4(b). This hyper-spherical arc makes an angle ϕ with v in the parameter space, as shown in Fig. 2(b). Surface-area of the spherical-cap is obtained by integrating (D-1) sphere of radius $r\sin\rho$ with arc element $rd\rho$ over the angle 0 to ϕ,

$$\begin{aligned} A_D^{Cap}(r) &= \int_0^{\phi} A_{D-1}(r\sin\rho)^{D-2} r d\rho \qquad (13) \\ &= \frac{2\pi^{\frac{D-1}{2}}}{\gamma(\frac{D-1}{2})} r^{D-1}\int_0^{\phi}\sin^{D-2}\rho d\rho \qquad (14) \\ &= \frac{1}{2}A_D(r) I_{\sin^2\phi}\left(\frac{D-1}{2},\frac{1}{2}\right) \qquad (15) \end{aligned}$$

where A_D is the total surface area of a D dimensional hyper-sphere and $I_*(.,.)$ is the regularized incomplete beta function. Also, $sin^2\phi$ could be expressed as $sin^2(tan^{-1}\sqrt{\eta})$ where $\eta = \frac{\alpha}{\theta}$ and thus,

$$A_D^{Cap}(r) = \frac{1}{2}A_D(r) I_{\sin^2(\tan^{-1}\sqrt{\eta})}\left(\frac{D-1}{2},\frac{1}{2}\right) \tag{16}$$

Since the solid angle spanned by the hyper ellipsoid is on either side of the origin and spans an equal solid angle of Ω_D in the $-v$ direction the surface area occupied by each code word is given by $2A_D^{cap}(r)$ and the maximum number of code words that fill the entire surface area is given by,

$$\begin{aligned} M_1 &= \frac{A_D(r)}{2A_D^{cap}(r)} \\ &= \frac{1}{I_{\sin^2(\tan^{-1}\sqrt{\eta})}\left(\frac{D-1}{2}, \frac{1}{2}\right)} \end{aligned} \tag{17}$$

and the capacity is given by,

$$C = \log_2 M_1 = \log_2\left(\frac{1}{I_{\sin^2(\tan^{-1}\sqrt{\eta})}\left(\frac{D-1}{2}, \frac{1}{2}\right)}\right) \tag{18}$$

Note that this value is dependent only on dimensions, the choice of ϕ and is independent of SNR.

This result was extended for a generic case, where $v = [v_1, v_2, ..., v_D]$, $\sum_{i=1}^{D} v_i = k$ with $v_i \in \{0, 1\} \, \forall \, i = [1, D]$, and similar to the BER_k result as shown in equation. 7 the capacity is given by estimating number of decoding cylinders on a D-k spherical surface and is given by

$$C = \log_2 M_k = \log_2\left(\frac{1}{I_{\sin^2(\tan^{-1}\sqrt{\eta})}\left(\frac{D-k}{2}, \frac{1}{2}\right)}\right) \tag{19}$$

4.3 Optimal decoding threshold for VBL.

For a given signal power and dimension, (SNR, D) pair, goal is to find the optimal parameter values (θ, α) or (θ', η) that would maximize both probability of correctness and the number of codewords in the signal space (p_d, M).

For the case of simple 1D representation, the error probabilities were asymmetric and are given by

$$p_{0|1} = \text{erfc}(\frac{\theta}{\sqrt{2}\sigma_0}) \tag{20}$$

$$p_{1|0} = 1 - \text{erfc}(\frac{\theta}{\sqrt{2}\sigma_1}) \tag{21}$$

where θ is the threshold, erfc(.) is the error function and σ_0, σ_1 are respective standard deviations representing 0 or 1. Thus average probability of error is given by,

$$BER_1 = p_1 p_{0|1} + p_0 p_{1|0} \tag{22}$$

$$= \frac{1}{2}\left[\text{erfc}(\frac{\theta}{\sqrt{2}\sigma_0}) + 1 - \text{erfc}(\frac{\theta}{\sqrt{2}\sigma_1})\right]. \tag{23}$$

Optimal Threshold in this case is determined by,

$$\min_\theta BER_1 = \min_\theta \frac{1}{2}\left[\text{erfc}(\frac{\theta}{\sqrt{2}\sigma_0}) + 1 - \text{erfc}(\frac{\theta}{\sqrt{2}\sigma_1})\right] \tag{24}$$

Taking derivative w.r.t θ and equating it to zero we get,

$$\theta_{opt} = \sqrt{\frac{2\sigma_0^2\sigma_1^2 \ln(\sigma_1/\sigma_0)}{\sigma_1^2 - \sigma_0^2}}. \tag{25}$$

The second derivative test shows that θ_{opt} gives the minimum probability of error for any given snr (σ_0, σ_1).

Acknowledgements

This work was supported in part by a research grant from the National Science Foundation CNS1646380.

References

[1] C. E. Shannon, "A mathematical theory of communication", *ACM SIGMOBILE Mobile Computing and Communications Review* **5** (2001) 3–55.

[2] S. H. Kondapalli, X. Zhang and C. Shantanu, "Variance-based digital logic for energy harvesting internet-of-things", in *IEEE Symposium on Circuits and Systems (ISCAS)* (IEEE, 2017).

[3] L. B. Kish, "Noise-based logic: Binary, multi-valued, or fuzzy, with optional superposition of logic states", *Physics Letters A* **373** (2009) 911–918.

[4] H. Dery, P. Dalal, L. Sham et al., "Spin-based logic in semiconductors for reconfigurable large-scale circuits", *Nature* **447** (2007) 573.

[5] H. A. Fahmy and R. A. Kiehl, "Complete logic family using tunneling-phase-logic devices", in *Microelectronics, 1999. ICM'99. The Eleventh International Conference on* (IEEE, 1999), pp. 153–156.

[6] K. Sri Harsha, Z. Xuan and C. Shantanu, "Energy-dissipation limits in variance-based computing", (World Scientific, 2018), volume 17, p. 1850013.

[7] L. B. Kish, "Thermal noise driven computing", *Applied Physics Letters* **89** (2006) 144104.

[8] S. Li, "Concise formulas for the area and volume of a hyperspherical cap", *Asian Journal of Mathematics and Statistics* **4** (2011) 66–70.

[9] J. Hamkins, *Design and analysis of spherical codes* (University of Illinois at Urbana-Champaign, 1996).

[10] C. E. Shannon, "Communication in the presence of noise", *Proceedings of the IRE* **37** (1949) 10–21.

[11] L. Gammaitoni, P. Hänggi, P. Jung and F. Marchesoni, “Stochastic resonance”, *Reviews of modern physics* **70** (1998) 223.

[12] C. E. Nebel, “Valleytronics: Electrons dance in diamond”, *Nature materials* **12** (2013) 690.

[13] R. Landauer, “Energy requirements in communication”, *Applied physics letters* **51** (1987) 2056–2058.

[14] L. B. Kish, R. Mingesz and Z. Gingl, “Thermal noise informatics: totally secure communication via a wire, zero-power communication, and thermal noise driven computing”, in *Noise and Fluctuations in Circuits, Devices, and Materials* (International Society for Optics and Photonics, 2007), volume 6600, p. 660003.